

Measuring Information Transfer Between Nodes in a Brain Network through Spectral Transfer Entropy

Paolo Victor Redondo*, Raphaël Huser**, and Hernando Ombao***

King Abdullah University of Science and Technology (KAUST), Thuwal 23955-6900, Saudi Arabia

**email*: paolovictor.redondo@kaust.edu.sa

***email*: raphael.huser@kaust.edu.sa

****email*: hernando.ombao@kaust.edu.sa

SUMMARY: Brain connectivity reflects how different regions of the brain interact during performance of a cognitive task. In studying brain signals such as electroencephalograms (EEG), this may be explored via Granger causality (GC) which tests if knowledge of the past values of a channel improves predictions on future values of another channel. However, the common approach to investigating GC is the vector autoregressive (VAR) model which is limited only to linear lead-lag relations. An alternative information-theoretic causal measure, transfer entropy (TE), becomes more appropriate since it does not impose any distributional assumption on the variables and covers any form of relationship (beyond linear) between them. To improve utility of TE in brain signal analysis, we propose a novel methodology to capture cross-channel information transfer in the frequency domain. Specifically, we introduce a new measure, the *spectral transfer entropy (STE)*, to quantify the magnitude and direction of information flow from a certain frequency-band oscillation of a channel to an oscillation of another channel. In contrast with previous works on TE in the frequency domain, we differentiate our work by considering the magnitude of filtered series (frequency band-specific), instead of using the spectral representation (frequency-specific) of a series. The main advantage of our proposed approach is that it allows adjustments for multiple comparisons to control family-wise error rate (FWER). One novel contribution is a simple yet efficient estimation method based on vine copula theory that enables estimates to capture zero (boundary point) without the need for bias adjustments. We showcase the advantage of our proposed measure through some numerical experiments and provide interesting and novel findings on the analysis of EEG recordings linked to a visual task.

KEY WORDS: Electroencephalogram; Frequency-band analysis; Mutual information; Transfer Entropy; Vine copula models.

1 Introduction

Establishing causal relationships between neural signals plays a huge role in understanding brain connectivity. During performance of a cognitive task, causality reflects the direction of information transfer taking place across nodes in the entire brain network. Granger causality (GC) is a widely-used causal inference framework for such dynamic systems. Given two time series X and Y , the notion of “ X Granger-causes Y ” implies that the variance of the predictions for Y improves by considering the past values of another series X together with its own history (Granger, 1963, 1969). Since GC suggests a directional relationship, it offers a nice foundation for exploring information transfer between signals coming from different brain regions.

Despite its well-built theoretical justifications, several restrictive assumptions (e.g., linearity and additivity) pose issues in the application of GC in neuroimaging data (Shojaie and Fox, 2022). Conceptualized by Schreiber (2000), an alternative approach that overcomes these limitations is through the concept of transfer entropy. Transfer entropy (TE) is an information-theoretic causal measure that quantifies the dependence between a series Y_t and the history of another series X_t given its own past values. Being equivalent to conditional mutual information (CMI), another dependence measure in information theory, TE shares the same properties as CMI. For example, the interpretation of “zero” TE from X_t to Y_t implies independence of Y_t on the lagged values of X_t given its own lagged values. Moreover, in addition to the congruence of TE and GC under Gaussianity (Barnett et al., 2009), TE does not assume any type of relationship between the series or impose any assumption on the distribution of the series. This makes TE a more general causal measure that is more suitable in analyzing connectivity in brain data like electroencephalograms (EEGs).

In EEG analysis, a common objective is to perform inference on the signals that are decomposed/filtered into different frequency bands (e.g., delta (0.5–4 Hz), theta (4–8 Hz),

alpha (8–12 Hz), beta (12–30 Hz), and gamma (30–100 Hz)) (Ombao et al., 2005; Nunez et al., 2016; Guerrero et al., 2021) which have well-known associated cognitive functions (Harmony, 2013; Bjørge and Emaus, 2017). To increase the applicability of TE in neuroscience, its development in the frequency domain becomes relevant. Recent efforts in this interest avoid the use of filtering (frequency band-specific) due to its effect of temporal dependence distortion and inability to isolate spectral causality (Barnett et al., 2009; Barnett and Seth, 2011), thus, implementing their methodologies on the spectral representations of the series (frequency-specific). Chen et al. (2019) embedded the phase-space reconstruction method with the two-dimensional Fourier transform while Tian et al. (2021) derived the theory for using wavelet transformation on the signals before calculating TE. However, these frequency-specific approaches may result in two possible drawbacks; increased family-wise error rate (FWER) in detecting significant spectral causal influence and vague practical interpretations.

Given that frequency-specific methods estimate TE for large number of possible frequencies in $(0, 0.5)$ and for multiple pairs of signal sources, detected significant quantities may be inappropriate after adjusting for multiple comparisons. Also, if the method employs computational techniques for testing significance (such as resampling), it is expected to suffer as the requirement for the number of replicates per test greatly increases with the number of simultaneous comparisons being tested (to ensure acceptable precision). Furthermore, suppose a significant TE is calculated only at a specific frequency in the boundary of two frequency bands, linking these results to established findings may become subjective. Since both issues can potentially minimize the method’s utility for clinicians and neuroscientists, we pursue the use of frequency band-specific filtered signals in developing TE in the frequency domain to attain an easy-to-interpret methodology that allows for controlling the FWER in the brain connectivity analysis.

In this paper, we propose a novel approach to quantify the amount and direction of

information transfer between two time series in the frequency domain. Instead of directly calculating TE between two filtered band-specific signals, we develop a new spectral causal measure, which we call the *spectral transfer entropy (STE)*, based on the magnitude of the filtered series. To minimize the impact of having different marginal distributions in estimation, we exploit the relationship, proven by Ma and Sun (2011), between copula theory and the information-theoretic measure. More specifically, an estimation procedure via vine copula models is introduced after expressing TE in terms of copula densities. By strategically arranging the variables in a D-vine structure, we show a simpler re-expression for calculating TE which is capable of capturing the boundary value of zero. Moreover, since resampling from an estimated copula can be done easily, a convenient bootstrap method for measuring uncertainty of the estimates is implemented which can readily accommodate correction for multiple comparisons.

The remainder of this paper is organized as follows. Section 2 provides a brief review of copula theory, dependence measures in information theory and their established equivalence. In Section 3, we define the new causal measure in the frequency domain, the STE, and its estimation based on vine copula models. To provide evidence on the performance of STE in capturing spectral influence, in Section 4, we use the proposed metric on some simulated series and on actual EEG recordings where we report interesting findings and novel results that describes the brain functional connectivity during performance of a visual task. Lastly, some concluding notes and future directions of our work are discussed in Section 6.

2 Quantifying Dependence via Copula Theory and Information Theory

Suppose that \mathbf{X} is a d -dimensional random vector where $F(\mathbf{x})$ and $f(\mathbf{x})$ represent its cumulative distribution function (CDF) and probability density function (PDF), respectively. Similar notations are used for other random vectors when the necessity occurs. Here, we present two concepts that quantify dependence between variables, namely, copula theory and

information theory. We first describe both concepts based on general random vectors but establish their relationship in the context of time series data afterwards. Then, we propose a novel estimation procedure for TE based on this link through vine copula models.

2.1 Copula Theory and the D-vine Structure

For any d -dimensional CDF F with univariate margins F_1, \dots, F_d , Sklar's theorem (Sklar, 1959) states that there exists a d -dimensional copula C such that

$$F(\mathbf{x}) = C\{F_1(x_1), \dots, F_d(x_d)\}, \quad \mathbf{x} \in \mathbb{R}^d. \quad (1)$$

An implication of Equation (1) is that, if the CDF F is absolutely continuous, then the joint PDF f can be expressed as

$$f(\mathbf{x}) = c\{F_1(x_1), \dots, F_d(x_d)\} \prod_i^d f_i(x_i), \quad (2)$$

where $c(\cdot)$ is the corresponding copula density. By Equation (2), the dependence structure of any jointly-distributed continuous random variables can be extracted independently from the marginal distributions. Such representation allows for a framework to describe the relationship between neural signals without dealing with the different marginal characteristics of the signals. Furthermore, Aas et al. (2009) showed that any d -dimensional copula density can be decomposed as product of bivariate copula and conditional bivariate copula. Although the decomposition is not unique, a graphical method, called regular vines, offers a systematic approach for the decomposition (Bedford and Cooke, 2001).

In this work, we focus on a specific vine structure called the D-vine (Aas et al., 2009). Assuming a D-vine structure, any d -dimensional copula density $c(F_1(x_1), \dots, F_d(x_d))$ can be written as

$$c(F_1(x_1), \dots, F_d(x_d)) = \prod_{j=1}^{d-1} \prod_{i=1}^{d-j} c(F(x_i|x_{i+1}, \dots, x_{i+j-1}), F(x_{i+j}|x_{i+1}, \dots, x_{i+j-1})). \quad (3)$$

By strategically organizing the arrangement of variables in a D-vine, the copula density of

any subset $\{X_{j_1}, \dots, X_{j_n} \mid j_1, \dots, j_n \in \{1, \dots, d\}, n \leq d\}$ can be obtained from Equation (3) by extracting the corresponding bivariate copula terms. With this, computations for some information-theoretic measures are simplified, which we exploit in our proposed estimation procedure for TE.

2.2 Mutual Information and Transfer Entropy

On the other hand, mutual information (MI) is the key formulation of dependence in information theory. More formally, the mutual information between two random vectors \mathbf{X} and \mathbf{Y} , denoted by $I(\mathbf{X}, \mathbf{Y})$ is defined as

$$\begin{aligned} I(\mathbf{X}, \mathbf{Y}) &= \int_{\mathbf{y}} \int_{\mathbf{x}} f(\mathbf{x}, \mathbf{y}) \log \frac{f(\mathbf{x}, \mathbf{y})}{f(\mathbf{x})f(\mathbf{y})} d\mathbf{x}d\mathbf{y} \\ &= D_{KL}(f(\mathbf{x}, \mathbf{y}) || f(\mathbf{x})f(\mathbf{y})) \end{aligned} \quad (4)$$

where $D_{KL}(P_X || P_Y)$ is the Kullback-Leibler divergence of the distribution P_X with respect to P_Y . In broad terms, MI is a measure of statistical dependence which calculates the discrepancy of the true joint probability model from the statistically independent model. Clearly, $I(\mathbf{X}, \mathbf{Y}) = 0$ if and only if \mathbf{X} and \mathbf{Y} are independent. Since MI does not impose any assumptions on the distribution of the random vectors or the form of relationship between them, it is the most general dependence measure (Ince et al., 2017). Additionally, considering another random vector \mathbf{Z} that affects the dependence between two random vectors, conditional mutual information (CMI) can be explored instead. The conditional mutual information between \mathbf{X} and \mathbf{Y} given \mathbf{Z} , denoted by $I(\mathbf{X}, \mathbf{Y} | \mathbf{Z})$, is given by

$$\begin{aligned} I(\mathbf{X}, \mathbf{Y} | \mathbf{Z}) &= \int_{\mathbf{z}} f(\mathbf{z}) \left[\int_{\mathbf{y}} \int_{\mathbf{x}} f(\mathbf{x}, \mathbf{y} | \mathbf{z}) \log \frac{f(\mathbf{x}, \mathbf{y} | \mathbf{z})}{f(\mathbf{x} | \mathbf{z})f(\mathbf{y} | \mathbf{z})} d\mathbf{x}d\mathbf{y} \right] d\mathbf{z} \\ &= \int_{\mathbf{z}} \int_{\mathbf{y}} \int_{\mathbf{x}} f(\mathbf{x}, \mathbf{y}, \mathbf{z}) \log \frac{f(\mathbf{z})f(\mathbf{x}, \mathbf{y}, \mathbf{z})}{f(\mathbf{x}, \mathbf{z})f(\mathbf{y}, \mathbf{z})} d\mathbf{x}d\mathbf{y}d\mathbf{z}. \end{aligned} \quad (5)$$

As CMI also takes its roots from the Kullback-Leiber divergence, it share the same properties as MI with application to conditional independence (see Gray (2011) for a more in-depth discussion). However, both MI and CMI are symmetric measures, i.e., $I(\mathbf{X}, \mathbf{Y}) = I(\mathbf{Y}, \mathbf{X})$

and $I(\mathbf{X}, \mathbf{Y}|\mathbf{Z}) = I(\mathbf{Y}, \mathbf{X}|\mathbf{Z})$. Hence, they do not indicate any direction of dependence. To formulate a congruent information-theoretic causal inference metric for time series, Schreiber (2000) developed the concept of transfer entropy.

Transfer entropy (TE) from a series Y_t to another series X_t , denoted by $TE(Y \rightarrow X; k, \ell)$, is the CMI between X_t and \mathbf{Y}_{t-k} given $\mathbf{X}_{t-\ell}$ where $\mathbf{Y}_{t-k} = (Y_{t-1}, \dots, Y_{t-k})^T$ and $\mathbf{X}_{t-\ell} = (X_{t-1}, \dots, X_{t-\ell})^T$. Mathematically,

$$\begin{aligned} TE(Y \rightarrow X; k, \ell) &= I(X_t, \mathbf{Y}_{t-k} | \mathbf{X}_{t-\ell}) \\ &= \int_{\mathbf{x}'} \int_{\mathbf{y}'} \int_{\mathcal{X}} f(x, \mathbf{x}', \mathbf{y}') \log \frac{f(\mathbf{x}') f(x, \mathbf{x}', \mathbf{y}')}{f(x, \mathbf{x}') f(\mathbf{x}', \mathbf{y}')} dx d\mathbf{y}' d\mathbf{x}'. \end{aligned} \quad (6)$$

In other words, $TE(Y \rightarrow X; k, \ell)$ measures the impact of the lagged values \mathbf{Y}_{t-k} on the series X_t given its own history $\mathbf{X}_{t-\ell}$ which is conceptually similar to GC. Also, TE shares the same properties as CMI. Moreover, Barnett et al. (2009) showed the equivalence of TE and GC under the Gaussianity assumption.

Additionally, the link between copula theory and information theory provides an efficient approach for estimating MI and CMI (which also applies to TE). By expressing the joint probability distribution with the corresponding copula density in Equation (2) and some change of variables in the integration, Ma and Sun (2011) showed that MI is related to copula entropy. We use the same technique for TE, viewed as CMI, to obtain the following:

$$TE(Y \rightarrow X; k, \ell) = \int_{[0,1]^{k+\ell+1}} c(u_x, \mathbf{u}_{\mathbf{x}'}, \mathbf{u}_{\mathbf{y}'}) \log \frac{c(\mathbf{u}_{\mathbf{x}'}) c(u_x, \mathbf{u}_{\mathbf{x}'}, \mathbf{u}_{\mathbf{y}'})}{c(u_x, \mathbf{u}_{\mathbf{x}'}) c(\mathbf{u}_{\mathbf{x}'}, \mathbf{u}_{\mathbf{y}'})} du_x d\mathbf{u}_{\mathbf{y}'} d\mathbf{u}_{\mathbf{x}'}, \quad (7)$$

where $u_x = F(x_t)$, $\mathbf{u}_{\mathbf{x}'} = (F(x_{t-1}), \dots, F(x_{t-\ell}))^T$ and $\mathbf{u}_{\mathbf{y}'} = (F(y_{t-k}), \dots, F(y_{t-1}))^T$. Hence, TE estimation requires only two steps: copula estimation and integration. The latter step is straightforward since many numerical methods are available, e.g., Monte Carlo integration. For the former, common techniques for estimating copula densities may be used, e.g., empirical copulas based on ranks or some parametric multivariate copulas. Thus, TE, together with its copula representation, offers a more general and appropriate framework for causal inference in neural signals with less restrictive assumptions.

3 Spectral Transfer Entropy

Here, we bridge TE to causal inference in neural signals. Although TE can provide evidence of significant information flow between nodes in a brain network, it does not specify from which oscillations the information is being transferred from and flows to. As a solution, we construct TE in the frequency domain through a new spectral dependence measure called *spectral transfer entropy (STE)*. Let Y_t and X_t to be the EEG recording at time t of two channels Y and X , $t = 1, \dots, T$. For $\Omega_1, \Omega_2 \in \{\delta, \theta, \alpha, \beta, \gamma\}$, denote by $Z_{Y,t}^{\Omega_1}$ and $Z_{X,t}^{\Omega_2}$ the oscillatory component of Y_t and X_t that are associated with the frequency bands Ω_1 and Ω_2 , respectively. The objective here is to infer the causal impact of $Z_{Y,t}^{\Omega_1}$ on $Z_{X,t}^{\Omega_2}$ (and vice versa) which is offered by the STE.

The spectral transfer entropy from an oscillatory component $Z_{Y,t}^{\Omega_1}$ of Y_t to the oscillatory component $Z_{X,t}^{\Omega_2}$ of X_t , denoted by $STE_{\Omega_1, \Omega_2}(Y \rightarrow X; k, \ell)$, is defined as

$$\begin{aligned} STE_{\Omega_1, \Omega_2}(Y \rightarrow X; k, \ell) &= TE(Z_Y^{\Omega_1} \rightarrow Z_X^{\Omega_2}; k, \ell) \\ &= I(Z_{X,t}^{\Omega_2}, \mathbf{Z}_{Y,t-k}^{\Omega_1} | \mathbf{Z}_{X,t-\ell}^{\Omega_2}). \end{aligned} \tag{8}$$

By its definition, STE enjoys all the nice properties of TE and CMI. It quantifies the amount of information transferred from a band-specific oscillation of a series to a certain oscillation of another series. More importantly, having zero STE implies that one oscillatory component does not have a spectral causal influence to the other. Hence, STE bridges TE to the frequency domain.

However, since $Z_{Y,t}^{\Omega_1}$ and $Z_{X,t}^{\Omega_2}$ are unobservable latent processes, estimation of STE requires extraction of these oscillatory components from the observed signals. One way to do this is by filtering. To avoid the well-known issue of the effect of filtering on causal inference in the frequency domain (temporal dependence distortion and false extraction of spectral influence) (see Barnett et al. (2009); Barnett and Seth (2011)), we suggest a simple ‘‘remedy’’ before

estimating TE on the filtered signals. Precisely, we perform the spectral causal inference based on STE as follows:

- (1) To extract the contribution of the five standard frequency bands, we apply a one-sided bandpass filter (Butterworth or finite impulse response (FIR)) on both Y_t and X_t .
- (2) Instead of using the filtered signals directly for estimation, we consider the magnitude (absolute value) of the band-specific series and denote them as $Y_t^{\Omega_1}$ and $X_t^{\Omega_2}$ for $\Omega_1, \Omega_2 \in \{\delta, \theta, \alpha, \beta, \gamma\}$.
- (3) Serving as substitutes for the oscillatory components $Z_{Y,t}^{\Omega_1}$ and $Z_{X,t}^{\Omega_2}$, we estimate STE based on $Y_t^{\Omega_1}$ and $X_t^{\Omega_2}$ using the proposed TE estimation in Section 3.1 and perform standard resampling methods for significance testing.
- (4) Since multiple connections are being tested simultaneously, we apply the Bonferroni correction on the bootstrap p-values to control for the FWER.

To highlight, our approach uses the magnitude of the filtered series instead of the actual values. That is, instead of focusing on the temporal characteristics of the filtered series, we compute STE based on the distribution of amplitudes, which is proportional to the frequency bands' spectral power. Hence, the proposed approach is robust to the issues of filtering in causal inference. Moreover, with finite number of frequency bands, controlling for FWER becomes feasible unlike for other frequency-specific methods – even when considering multiple channel pairs in the brain network.

On the other hand, the magnitudes of the band-specific signals are expected to have different marginal characteristics due to the difference in contribution to the original series. Thus, computation for STE benefits by using the copula-based estimation for TE.

3.1 Novel Copula-based Estimation for Transfer Entropy

Using common d -dimensional copulas, such as the elliptical copulas and Archimedean copulas, limits the type of dependence each subset pair of variables can exhibit. For example,

assuming a multivariate normal copula forces no tail dependence between all variables while a multivariate Gumbel copula induces only upper tail dependence. Such limitation is addressed by the sequential estimation approach proposed by Aas et al. (2009) where the pair copulas that consists the decomposition of the d -dimensional copula are modelled separately. This allows for a more flexible specification of the pairwise relationship between the variables as different copula families may be selected for each pair copula. In addition, by strategically arranging the variables as $(X_t, X_{t-1}, \dots, X_{t-\ell}, Y_{t-k}, \dots, Y_{t-1})^T$ (equivalently, as $(u_x, \mathbf{u}_{\mathbf{x}'}, \mathbf{u}_{\mathbf{y}'})^T$) in a D-vine structure, we further simplify the calculation for TE. More concretely, because the $c(\mathbf{u}_{\mathbf{x}'})$, $c(u_x, \mathbf{u}_{\mathbf{x}'})$, and $c(\mathbf{u}_{\mathbf{x}'}, \mathbf{u}_{\mathbf{y}'})$ are “subsets” of the full joint copula density, by expressing them into their corresponding D-vine decomposition, some common factors cancel out in the log component of $TE(Y \rightarrow X; k, \ell)$ (see Figure 1). To illustrate this, suppose $k, \ell = 2$. The copula densities $c(u_x, \mathbf{u}_{\mathbf{x}'}, \mathbf{u}_{\mathbf{y}'})$, $c(\mathbf{u}_{\mathbf{x}'})$, $c(u_x, \mathbf{u}_{\mathbf{x}'})$ and $c(\mathbf{u}_{\mathbf{x}'}, \mathbf{u}_{\mathbf{y}'})$, based on the D-vine, can be represented as follows:

$$\begin{aligned}
c(u_x, \mathbf{u}_{\mathbf{x}'}, \mathbf{u}_{\mathbf{y}'}) &= c(F(x_t), F(x_{t-1}))c(F(x_{t-1}), F(x_{t-2}))c(F(x_{t-2}), F(y_{t-2}))c(F(y_{t-2}), F(y_{t-1})) \\
&\quad \times c(F(x_t|x_{t-1}), F(x_{t-2}|x_{t-1}))c(F(x_{t-1}|x_{t-2}), F(y_{t-2}|x_{t-2})) \\
&\quad \times c(F(x_{t-2}|y_{t-2}), F(y_{t-1}|y_{t-2}))c(F(x_t|x_{t-1}, x_{t-2}), F(y_{t-2}|x_{t-1}, x_{t-2})) \\
&\quad \times c(F(x_{t-1}|x_{t-2}, y_{t-2}), F(y_{t-1}|x_{t-2}, y_{t-2})) \\
&\quad \times c(F(x_t|x_{t-1}, x_{t-2}, y_{t-2}), F(y_{t-1}|x_{t-1}, x_{t-2}, y_{t-2})) \\
c(\mathbf{u}_{\mathbf{x}'}) &= c(F(x_{t-1}), F(x_{t-2})) \\
c(u_x, \mathbf{u}_{\mathbf{x}'}) &= c(F(x_t), F(x_{t-1}))c(F(x_{t-1}), F(x_{t-2}))c(F(x_t|x_{t-1}), F(x_{t-2}|x_{t-1})) \\
c(\mathbf{u}_{\mathbf{x}'}, \mathbf{u}_{\mathbf{y}'}) &= c(F(x_{t-1}), F(x_{t-2}))c(F(x_{t-2}), F(y_{t-2}))c(F(y_{t-2}), F(y_{t-1})) \\
&\quad \times c(F(x_{t-1}|x_{t-2}), F(y_{t-2}|x_{t-2}))c(F(x_{t-2}|y_{t-2}), F(y_{t-1}|y_{t-2})) \\
&\quad \times c(F(x_{t-1}|x_{t-2}, y_{t-2}), F(y_{t-1}|x_{t-2}, y_{t-2}))
\end{aligned}$$

Thus, for $k, \ell = 2$, after cancellation of common factors,

$$\log \frac{c(\mathbf{u}_{\mathbf{x}'})c(u_x, \mathbf{u}_{\mathbf{x}'}, \mathbf{u}_{\mathbf{y}'})}{c(u_x, \mathbf{u}_{\mathbf{x}'})c(\mathbf{u}_{\mathbf{x}'}, \mathbf{u}_{\mathbf{y}'})} = \log \{ c(F(x_t|x_{t-1}, x_{t-2}), F(y_{t-2}|x_{t-1}, x_{t-2})) \\ \times c(F(x_t|x_{t-1}, x_{t-2}, y_{t-2}), F(y_{t-1}|x_{t-1}, x_{t-2}, y_{t-2})) \}$$

This simplified form based on the D-vine naturally aligns with the definition of TE, i.e., the remaining pair copulas reflect the relationship between the current value of one series to the past values of another series given its own history. In general, for any k and ℓ ,

$$\log \frac{c(\mathbf{u}_{\mathbf{x}'})c(u_x, \mathbf{u}_{\mathbf{x}'}, \mathbf{u}_{\mathbf{y}'})}{c(u_x, \mathbf{u}_{\mathbf{x}'})c(\mathbf{u}_{\mathbf{x}'}, \mathbf{u}_{\mathbf{y}'})} = \log \prod_{j=1}^k c(F(x_t|\mathbf{x}_{t-\ell}, \mathbf{y}_{t-(j+1)}), F(y_{t-j}|\mathbf{x}_{t-\ell}, \mathbf{y}_{t-(j+1)})), \quad (9)$$

where $\mathbf{x}_{t-\ell} = (x_{t-1}, \dots, x_{t-\ell})^T$ and $\mathbf{y}_{t-(j+1)} = (y_{t-(j+1)}, y_{t-(j+2)}, \dots, y_{t-k})^T$ with $\mathbf{y}_{t-(k+1)}$ removed from the conditioning set. As a result, the computation for TE only requires the remaining conditional bivariate copulas (not the full joint copula density). Hence, we estimate TE as follows:

- (1) For pre-specified k and ℓ , arrange the variables for the D-vine structure and transform them into the uniform scale based on ranks. Denote the proposed arrangement and transformed vector by

$$(x_t, x_{t-1}, \dots, x_{t-\ell}, y_{t-k}, \dots, y_{t-1}, y_t)^T \longrightarrow (u_x, \mathbf{u}_{\mathbf{x}'}, \mathbf{u}_{\mathbf{y}'}, u_y)^T,$$

where $u_x = \hat{F}(x_t)$, $\mathbf{u}_{\mathbf{x}'} = (\hat{F}(x_{t-1}), \dots, \hat{F}(x_{t-\ell}))^T$, $\mathbf{u}_{\mathbf{y}'} = (\hat{F}(y_{t-k}), \dots, \hat{F}(y_{t-1}))^T$, and $u_y = \hat{F}(y_t)$ with $\hat{F}(\cdot)$ is the empirical CDF.

- (2) Fit a vine copula model for $(u_x, \mathbf{u}_{\mathbf{x}'}, \mathbf{u}_{\mathbf{y}'}, u_y)^T$ using the sequential estimation procedure developed by Aas et al. (2009). That is, for each pair copula in the decomposition, we select the “best” bivariate copula family based on some information criterion (e.g., modified Bayesian information criterion for vines (mBICv) (Nagler et al., 2019)), and estimate the parameters of the chosen families. Choices for the bivariate copula selection may include the independence copula, elliptical copulas (Gaussian and Student’s t), and Archimedean copulas (Clayton, Frank, Gumbel and Joe).

- (3) From the estimated vine copula, using the equality in Equation (9) and Monte Carlo integration, the estimators for $TE(Y \rightarrow X; k, \ell)$ and $TE(X \rightarrow Y; \ell, k)$ are given by

$$\widehat{TE}(Y \rightarrow X; k, \ell) = \frac{\sum_{t=p+1}^T \log \prod_{j=1}^k \hat{c}(F(x_t | \mathbf{x}_{t-\ell}, \mathbf{y}_{t-(j+1)}), F(y_{t-j} | \mathbf{x}_{t-\ell}, \mathbf{y}_{t-(j+1)}))}{T - p},$$

and

$$\widehat{TE}(X \rightarrow Y; k, \ell) = \frac{\sum_{t=p+1}^T \log \prod_{j=1}^{\ell} \hat{c}(F(y_t | \mathbf{y}_{t-k}, \mathbf{x}_{t-(j+1)}), F(x_{t-j} | \mathbf{y}_{t-k}, \mathbf{x}_{t-(j+1)}))}{T - p},$$

respectively, where $p = \max\{k, \ell\}$ and the $\hat{c}(\cdot, \cdot)$ s are estimated pair copula densities. To emphasize, both estimated TEs are calculated from the same vine copula for $(u_x, \mathbf{u}_{\mathbf{x}'}, \mathbf{u}_{\mathbf{y}'}, u_y)^T$.

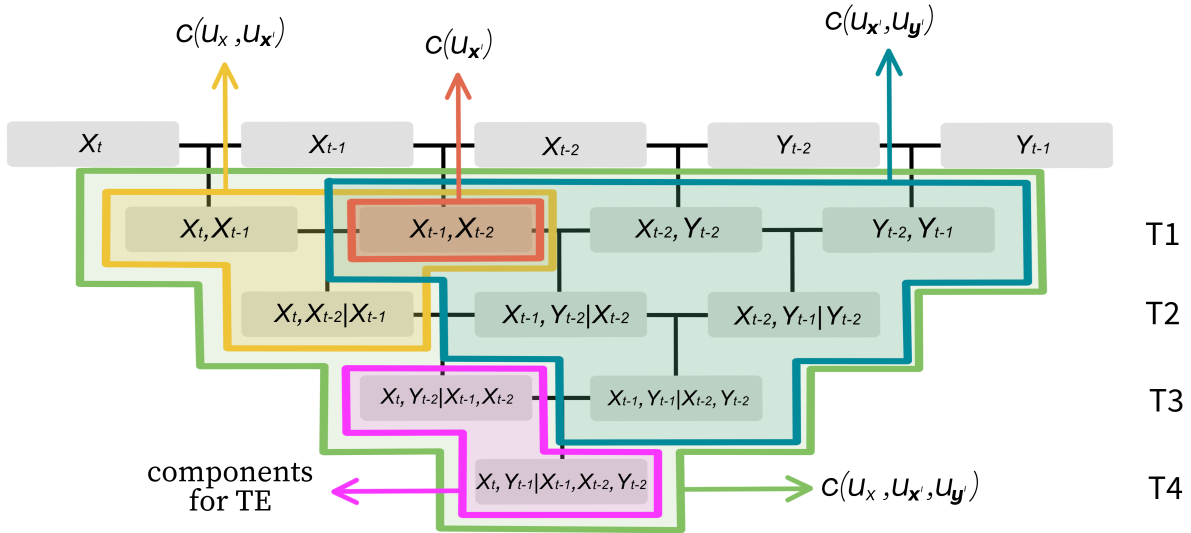


Figure 1. Illustration for calculating $TE(Y \rightarrow X; k = 2, \ell = 2)$ based on the strategically arranged D-vine copula structure of the original (X_t) and lagged series $(X_{t-1}, X_{t-2}, Y_{t-1}, Y_{t-2})$.

An advantage of our approach is its ability to provide estimates at the boundary point zero. Existing estimation procedures for TE requires “shuffling” to adjust the estimates from

the bias due to finite sample effects (Marschinski and Kantz, 2002). However, our method is robust to this problem. Whenever independent copulas are selected for the remaining conditional bivariate copula in Equation (9), the estimated TE attains an exact value of zero, thus, removing the necessity for bias adjustment. Hence, the new estimation scheme that we introduce provides a simple and efficient way for calculating TE.

3.2 A Resampling Method for Testing Significance of Transfer Entropy

Another benefit offered by our procedure is the convenience of measuring uncertainties of the estimates. Since new observations can be easily generated from an estimated vine copula model, standard resampling method works well with our estimation approach to compute for significance levels (p -values). Suppose we wish to test the following hypotheses:

$$H_0 : TE(Y \rightarrow X; k, \ell) = 0$$

$$\text{vs. } H_1 : TE(Y \rightarrow X; k, \ell) > 0.$$

Under the null hypothesis, $TE(Y \rightarrow X; k, \ell) = 0$ implies that the corresponding pair copulas $c(F(x_t|\mathbf{x}_{t-\ell}, \mathbf{y}_{t-(j+1)}), F(y_{t-j}|\mathbf{x}_{t-\ell}, \mathbf{y}_{t-(j+1)}))$, for $j = 1, \dots, k$, are all equal to the independence copula. This enables simulating observations under H_0 from the estimated vine copula $\hat{C}(u_x, \mathbf{u}_{\mathbf{x}'}, \mathbf{u}_{\mathbf{y}'}, u_y)$ based on the original data. Denote the vine copula model under the null hypothesis as $C^{(0)}(u_x, \mathbf{u}_{\mathbf{x}'}, \mathbf{u}_{\mathbf{y}'}, u_y)$. The pair copulas consisting $C^{(0)}(\cdot)$ are the same bivariate copulas from the estimated $\hat{C}(\cdot)$ except for the components that are associated with $TE(Y \rightarrow X; k, \ell)$ and $TE(X \rightarrow Y; \ell, k)$ which we replace by the independence copula (see Figure 2). Thus, new observations generated from the $C^{(0)}(\cdot)$ preserve the dependence structure within each observed series X and Y , but eliminates the information transfer between them. Repeatedly estimating TE from these generated observations then provides an empirical distribution of the estimator under the null hypothesis of no information transfer. Hence, we perform testing for significance of $TE(Y \rightarrow X; k, \ell)$ and $TE(X \rightarrow Y; \ell, k)$ based on the outline below:

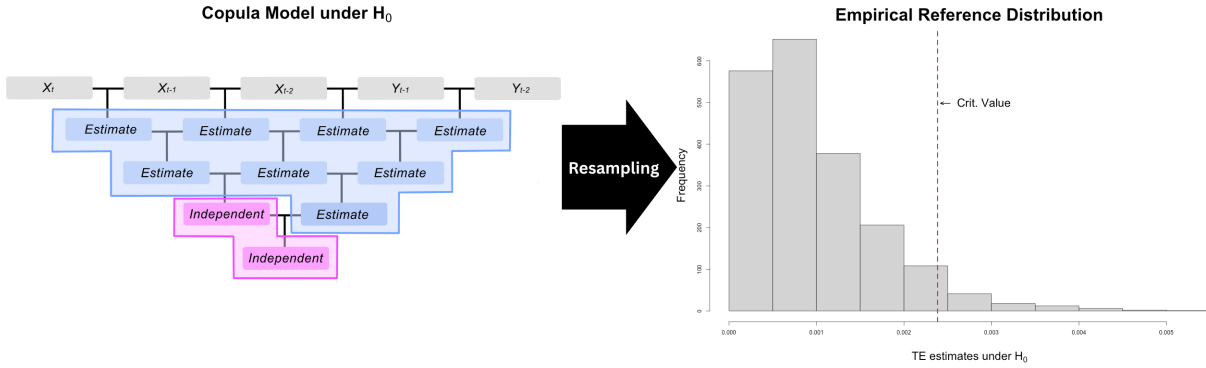


Figure 2. The copula model under the null hypothesis and the generated empirical reference distribution for hypothesis testing.

- (1) Generate new observations from the null vine copula model $C^{(0)}(\cdot)$ of the same length as the original data.
- (2) Estimate $TE(Y \rightarrow X; k, \ell)$ and $TE(X \rightarrow Y; \ell, k)$ from the new observations using the proposed copula-based estimation procedure and denote them by $\widehat{TE}^{(b)}(Y \rightarrow X; k, \ell)$ and $\widehat{TE}^{(b)}(X \rightarrow Y; \ell, k)$, respectively.
- (3) Compute the p -value for testing the significance of the original estimate $\widehat{TE}(Y \rightarrow X; k, \ell)$ as the relative frequency of the event $\{\widehat{TE}^{(b)}(Y \rightarrow X; k, \ell) \geq \widehat{TE}(Y \rightarrow X; k, \ell)\}$ among all resamples considered ($b = 1, \dots, B$). The p -value for $\widehat{TE}(X \rightarrow Y; \ell, k)$ requires similar computations.
- (4) Given a specified level of significance $\alpha \in (0, 1)$, reject the associated null hypothesis if the p -value is less than $\alpha/2$. Otherwise, do not reject H_0 .

Since TE from both directions are estimated from the same set of generated observations, we include the Bonferroni correction for simultaneously testing the significance of the two-way information transfer. This points to the efficiency of the proposed resampling scheme as a set of resampled data from the null model can be used to estimate both directions for TE and can easily adjust for multiple comparisons. Such feature is desirable in studying brain connectivity, especially when considering multiple pairs of nodes in a brain network while simultaneously taking into account several oscillatory components.

4 Numerical Experiments

In this section, we explore the capability of the proposed STE in capturing information transfer in the frequency domain through simulations. Particularly, we provide evidence on the validity of our estimation procedure in detecting significant and non-significant flow of information across different frequency oscillations and its advantages over the traditional Granger causality test. We generated several pairs of unit-variance latent processes (at sampling rate of 100 Hz) based on their respective AR(2) representations to mimic the five standard frequency bands: delta (0.5–4 Hz), theta (4–8 Hz), alpha (8–12 Hz), beta (12–30 Hz), and gamma (30–45 Hz). Denote $\{Z_1^\Omega(t), Z_2^\Omega(t)\}$ be the pair of latent processes coming from the frequency band Ω where $\Omega \in \{\delta, \theta, \alpha, \beta, \gamma\}$. Moreover, we induce dependence between the latent processes by specifying the following:

$$\text{Cov}\{Z_1^\Omega(t), Z_2^\Omega(t)\} = \begin{cases} 0.9, & \text{if } \Omega \in \{\theta, \beta\} \\ 0, & \text{if } \Omega \in \{\delta, \alpha, \gamma\} \end{cases} \quad (10)$$

In addition, we simulate the theta-gamma coupling phenomenon by modulating the amplitude of the gamma latent process with the magnitude of the theta latent process, i.e., $Z_3^\gamma(t) = \text{sgn}(Z_2^\gamma(t)) \times |Z_1^\theta(t)|$ where $\text{sgn}(x) = x/|x|$ for $x \neq 0$ (0 otherwise) (see Figure 3). Then, we define two series X_t and Y_t as a linear combination of the latent processes such that

$$\begin{aligned} X_t &= g\{Z_1^\delta(t), Z_1^\theta(t), Z_1^\alpha(t), Z_1^\beta(t), Z_1^\gamma(t), W_1(t)\} \\ Y_t &= h\{Z_2^\delta(t), Z_2^\theta(t), Z_2^\alpha(t), Z_2^\beta(t-2), Z_3^\gamma(t), W_2(t)\} \end{aligned} \quad (11)$$

where $g(\cdot)$ and $h(\cdot)$ are linear functions with coefficients summing to one, and $W_1(t), W_2(t) \stackrel{\text{iid}}{\sim} N(0, 1)$. With this specification, we expect five pairs of STE to be significant (namely $STE_{\theta, \theta}(X \rightarrow Y)$, $STE_{\theta, \theta}(Y \rightarrow X)$, $STE_{\beta, \beta}(Y \rightarrow X)$, $STE_{\theta, \gamma}(X \rightarrow Y)$ and $STE_{\gamma, \theta}(Y \rightarrow X)$) while the rest are non-significant.

Figure 4 shows the estimated TE for the original series and the STE for the filtered

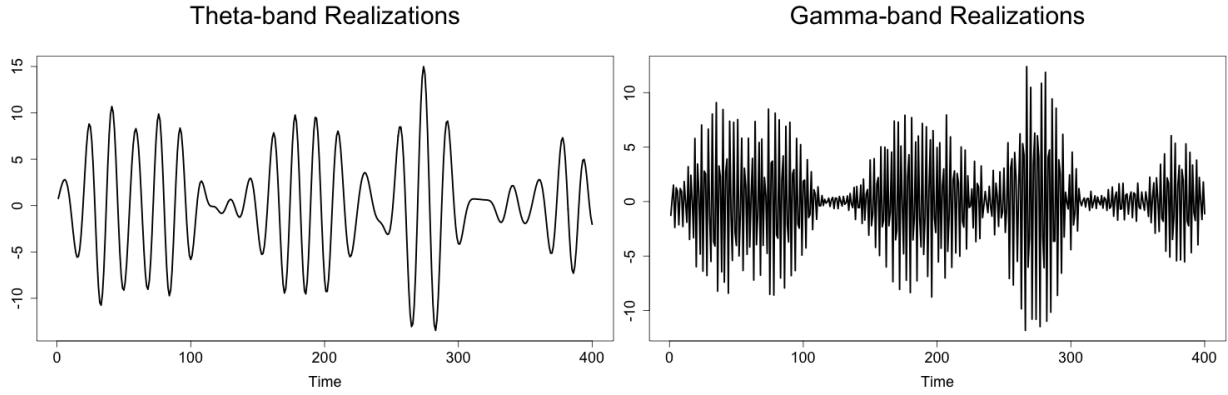


Figure 3. Simulated theta-gamma coupling phenomenon.

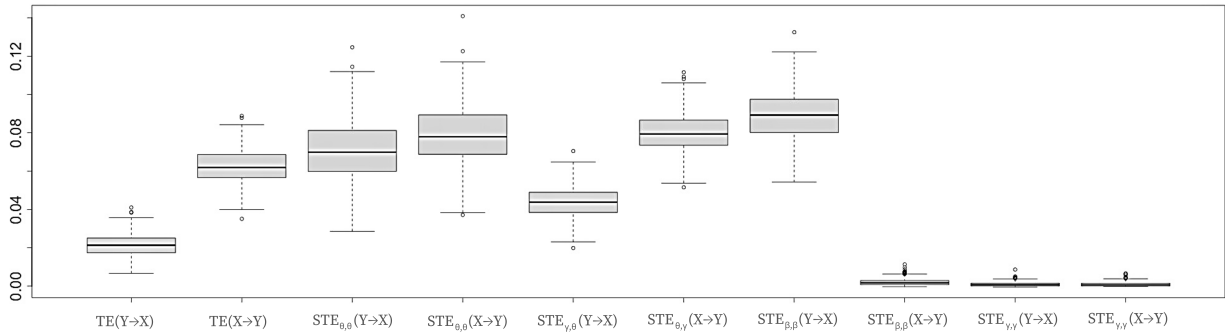


Figure 4. Estimated TE between the original series X_t and Y_t , and STE between the filtered frequency band-specific series $X_t^{\Omega_1}$ and $Y_t^{\Omega_2}$ for selected frequency bands Ω_1 and Ω_2 based from $B = 500$ replicates.

frequency band-specific series for $B = 500$ replicates. As a first step, we evaluate the global TE (i.e., without considering frequency-band specific oscillations). The estimated global TE effectively captures the flow of information between the two series as both direction ($X \rightarrow Y$ and $Y \rightarrow X$) are significant. However, this provides less information compared to STE. Since clinicians are often concerned about the impact of different frequency bands to one another, the advantage of STE becomes clear as it is able to detect significant links between the simulated frequency bands, even cross-frequency coupling (theta-gamma). It not only captures the significant information transfer, but it also properly detects non-significant STE, e.g., the STE in the beta band where $STE_{\beta,\beta}(Y \rightarrow X) > 0$ but $STE_{\beta,\beta}(X \rightarrow Y) = 0$.

Moreover, we compare our methodology with the traditional Granger causality test based

Table 1

Proportion of significant frequency band-specific causal link based on the standard GC test and the proposed STE metric from $B = 500$ replicates.

$Y \rightarrow X$	STE	GC	$X \rightarrow Y$	STE	GC
$\delta \rightarrow \delta$	0.072	0.130	$\delta \rightarrow \delta$	0.040	0.210
$\theta \rightarrow \theta$	1.000	1.000	$\theta \rightarrow \theta$	1.000	1.000
$\alpha \rightarrow \alpha$	0.074	0.790	$\alpha \rightarrow \alpha$	0.066	0.812
$\beta \rightarrow \beta$	1.000	1.000	$\beta \rightarrow \beta$	0.002	0.606
$\gamma \rightarrow \gamma$	0.000	0.098	$\gamma \rightarrow \gamma$	0.000	0.132
$\gamma \rightarrow \theta$	1.000	1.000	$\theta \rightarrow \gamma$	1.000	1.000

on a VAR($p = 2$) model of the filtered series. Table 1 shows the proportion of significant STE estimates for some selected pairs of frequency bands. The GC test based on the VAR($p = 2$) model assumes linearity in the effect of one series to the other, which rarely occur in actual applications. Because this assumption oversimplifies the structure at which the causality is tested, it becomes more prone to false detection. Thus, an advantage of the proposed STE metric over the traditional GC test is that it does not impose any assumption on the type of relationship between the two series which lessens the risk of detecting spurious dependence.

5 EEG Analysis: Brain Connectivity During a Visual Task

Now, we investigate brain connectivity by analyzing EEG recordings of children (one with attention deficit hyperactivity disorder (ADHD) and one without any registered psychiatric disorder (healthy control)) during performance of a visual task. The data, collected by Motie Nasrabadi et al. (2020), contains samples of EEGs at 128Hz, from 19 channels. To remove unwanted artifacts and increase the quality of the recordings, pre-processing was conducted via the PREP pipeline of Bigdely-Shamlo et al. (2015). Then, the pre-processed EEGs were standardized to a unified scale (zero-mean unit variance series). The visual-cognitive experiment was to count the number of characters in a flashed image. Hence, to “represent” brain regions that are highly likely to be engaged during the cognitive task, we selected six EEG channels, namely, Fp1 (left pre-frontal), Fp2 (right pre-frontal), T7 (left temporal), T8 (right temporal), O1 (left occipital) and O2 (right occipital) (see Figure 5b).

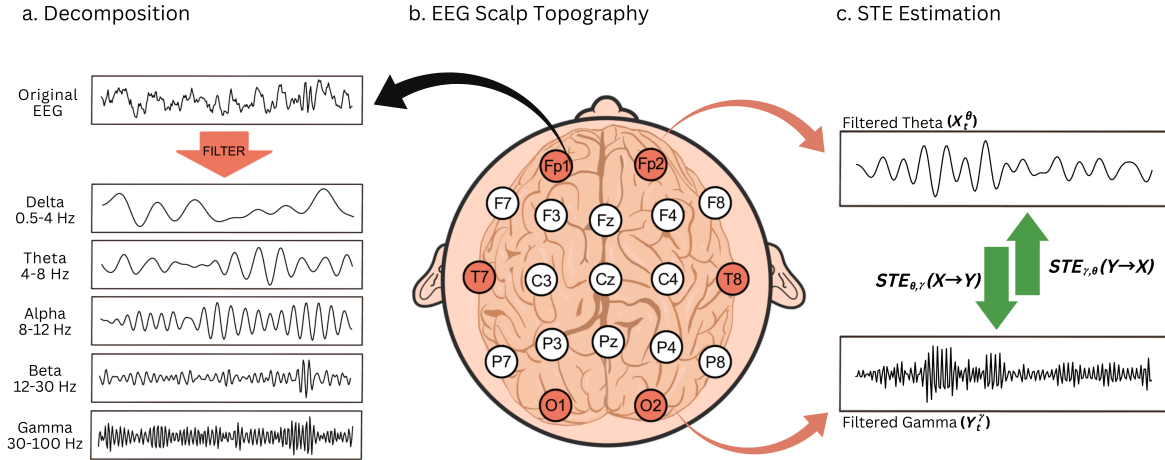


Figure 5. Building blocks of STE. (a) Application of bandpass filter on original EEG series to obtain frequency band-specific filtered series. (b) Standard 10-20 EEG scalp topography where the highlighted channels are included in the analysis. (c) Illustration for STE estimation between two filtered series.

Given that the frontal region is linked with concentration, focus and problem solving, the temporal region for speech and memory, and the occipital region for visual processing (Bjørge and Emaus, 2017), the interest now is to identify which cross-channel information transfer is significant and at which frequency bands it occurs.

Since the dataset does not indicate the time stamps at which the images are flashed, we employ a sliding window approach to capture the evolution of the thinking process during the experiment. Given the first 55-second segment of the EEG recordings for each subject, we consider overlapping time windows of length 10 seconds with overlap of five seconds between adjacent time windows. Arguably, this ensures that the series we use for estimating the STE are (locally) stationary. On the other hand, to obtain the filtered frequency band-specific series per channel, 4th order Butterworth band-pass filters are applied to the standardized and pre-processed EEG series (see Figure 5a). Then, we calculate the STE for each possible pair of the selected channels at each permutation of possible frequency bands (see Figure 5c). Tests for significance of the calculated magnitudes of the spectral information transfer are conducted based on $B = 2000$ bootstrap resamples. A total of 750 individual significance

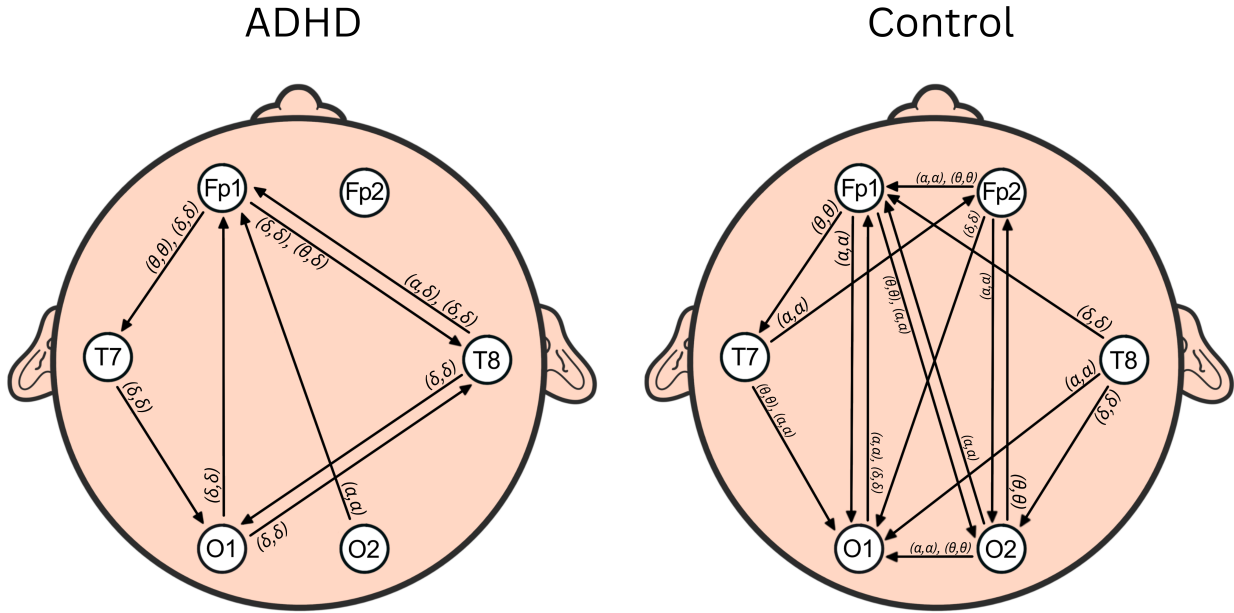


Figure 6. Derived brain connectivity network for the two subjects performing the visual task based on the STE with significant Bonferroni-adjusted p -values.

tests are implemented and their corresponding Bonferroni-adjusted p -values are used to describe the brain connectivity of the two subjects. To compare the results from our proposed STE metric, we also perform the GC test to the filtered series with correction for multiple comparisons.

Due to the large number of “significant” spectral information transfer detected by the standard GC test (even after adjusting for multiple comparison), we do not anymore show its derived brain connectivity network but rather, summarize its points. For every filtered frequency band-specific series, the derived network shows an almost fully connected graph, i.e., each channel transfers information to almost all channels at almost all frequency bands. This is true for both subjects across all considered time windows. As previously mentioned, since the GC test based on the $\text{VAR}(p = 2)$ model works under the assumption of linearity, oversimplification of the data structure may lead to detection of spurious causal relationship. Thus, the result of having an almost fully connected brain network may be misleading. On the other hand, Figure 6 provides the estimated brain connectivity network for each subject

based on the novel STE metric. Unlike the traditional GC test, our proposed method is able to detect fewer but meaningful cross-channel interactions.

Even though STE is a directional (causal) measure, our novel approach captures that some channels transfer information in a two-way manner. That is, different channels “communicate” due to having significant STEs from one direction and vice versa. For example, $Fp1(\alpha) \leftrightarrow O1(\alpha)$ and $Fp1(\alpha) \leftrightarrow O2(\alpha)$ are significant for the healthy control while $Fp1(\delta) \leftrightarrow T8(\delta)$ and $O1(\delta) \leftrightarrow T8(\delta)$ are evident for the subject with ADHD. We deem this finding highly plausible because the “thinking” process involved in counting characters does not happen in an instant, hence, requires a “continuous” two-way feedback connection/link between functioning channels.

The derived brain network for the healthy subject has prominent connections in the theta and alpha frequency bands which is associated with sustained attention and controlled access to stored information or memory (Knyazev, 2007; Klimesch, 2012; Behzadnia et al., 2017). In contrast, transferred information in the brain connectivity network of the subject with ADHD are dominantly in the delta oscillations. This is related to requiring attention to internal processing, i.e., selectively suppressing unnecessary or irrelevant neural activity to accomplish a mental task (Fernández et al., 1995; Harmony et al., 1996). The theta and alpha connections for the healthy control reflects the ability of the subject to maintain focus during performance of the visual task. Meanwhile, the delta connections for the subject with ADHD (and the scarcity of theta and alpha connections) provides evidence of having short attention span.

Moreover, compared to the healthy control, the subject with ADHD has less significant cross-channel information transfers. Specifically, we see minimal interaction with the occipital channels (visual processing) and the pre-frontal channels (problem solving) in the estimated brain network of the ADHD subject. Further, we see a significant “cycle” of information

flow in the delta band from the pre-frontal, temporal and occipital channels (Fp1 \rightarrow T7 \rightarrow O1 \rightarrow T8 \rightarrow Fp1). This is another indication of requiring attention to internal processing where visual inputs are stored and filtered in the temporal channels before being transferred to the problem solving (pre-frontal) channels. On the other hand, the brain network of the healthy control suggests direct links between the visual processing (occipital) channels and the problem solving channels. In addition, channels of the same cognitive function (i.e., Fp1 and Fp2, and O1 and O2) are connected in the theta and alpha band which reflects the efficiency in the thinking process of the healthy subject in performing the visual task.

6 Conclusion

During performance of a specific cognitive task, interactions between different brain regions occur in the form of information transfer. In EEG analysis, this phenomenon can be visualized through the magnitude of cross-channel information flow. Transfer entropy (TE), an information-theoretic measure, offers a general framework for quantifying the dependence of a specific channel on the past values of another channel given its own past. Given its property that a zero TE implies independence between the channel and the past of another, TE is considered to be a causal measure which we interpret as a measure of information transfer. As several brain functions are attributed to specific groups of frequency oscillations (frequency bands), application of TE in the frequency domain becomes more desirable. Thus, we propose a new metric called spectral transfer entropy (STE) by calculating TE on magnitude of filtered frequency band-specific signals.

The advantage of our proposed STE is that it provides the magnitude of information transfer from a specific oscillatory component of a series to another oscillatory component of another series. It yields higher utility to clinicians since its interpretations are directly linked to standard frequency bands, unlike other works on TE in the frequency domain (which are frequency-specific, not frequency band-specific). Furthermore, our proposed methodology

easily allows for adjustment for multiple comparisons which are often not addressed in its frequency-specific counterparts. With this, the risk of detecting spurious information transfer is not an issue since controlling for the family-wise error rate (FWER) is straightforward.

In addition, we propose a novel estimation method for TE/STE based on vine copula models. Given that TE can be expressed as conditional mutual information (CMI), calculations for TE are simplified by considering a D-vine copula structure for the full joint copula density. This results in a simpler and more efficient way of estimating TE/STE. Another advantage of our approach is that it is able to obtain a “zero” TE exactly, which removes the necessity to adjust the estimates for bias because of finite data (also known as “shuffling”). Moreover, measuring uncertainty of the estimates based on a bootstrap approach is fast because resampling from an estimated copula is often convenient.

Our novel STE measure provided interesting findings in the analysis of EEG data linked to a visual task. In contrast with the results of the standard Granger causality (GC) test which indicates excessively many difficult-to-interpret cross-channel connections, our proposed measure is able to provide fewer but meaningful links between nodes in a brain network for both the healthy control and subject with ADHD. Based on the results from the STE, significant information flow are prominent in the delta band for the ADHD subject which relates to requiring attention to internal processing. Meanwhile, transferred information in the estimated brain network of the healthy subject are dominantly found in the theta and alpha bands which translates to sustained attention and controlled access to stored information. With the significant information transfer between channels of similar associated cognitive functions ($Fp2 \rightarrow Fp1$, and $O2 \rightarrow O1$), the transferred information in the theta and alpha oscillations suggest the efficiency of the thinking process of the healthy subject in performing the visual task.

Lastly, the proposed STE measure considers the transfer of information in the bulk of the

distribution. This is a limitation because different amplitudes of a signal reflect different states of the brain. For example, high amplitude signals are associated with a more actively functioning state. Thus, looking at the transfer entropy in the tail of the distribution may provide further insights on brain connectivity. In future research, it would be interesting to develop the concept of “tail” transfer entropy, both in the time and frequency domains.

References

- Aas, K., Czado, C., Frigessi, A., and Bakken, H. (2009). Pair-copula constructions of multiple dependence. *Insurance: Mathematics and economics* **44**, 182–198.
- Barnett, L., Barrett, A. B., and Seth, A. K. (2009). Granger causality and transfer entropy are equivalent for gaussian variables. *Physical review letters* **103**, 238701.
- Barnett, L. and Seth, A. K. (2011). Behaviour of granger causality under filtering: theoretical invariance and practical application. *Journal of neuroscience methods* **201**, 404–419.
- Bedford, T. and Cooke, R. M. (2001). Probability density decomposition for conditionally dependent random variables modeled by vines. *Annals of Mathematics and Artificial Intelligence* **32**, 245–268.
- Behzadnia, A., Ghoshuni, M., and Chermahini, S. (2017). Eeg activities and the sustained attention performance. *Neurophysiology* **49**, 226–233.
- Bigdely-Shamlo, N., Mullen, T., Kothe, C., Su, K.-M., and Robbins, K. A. (2015). The prep pipeline: standardized preprocessing for large-scale eeg analysis. *Frontiers in neuroinformatics* **9**, 16.
- Bjørge, L.-E. N. and Emaus, T. H. (2017). Identification of eeg-based signature produced by visual exposure to the primary colors rgb. *no. July* .
- Chen, X., Zhang, Y., Cheng, S., and Xie, P. (2019). Transfer spectral entropy and application

- to functional corticomuscular coupling. *IEEE Transactions on Neural Systems and Rehabilitation Engineering* **27**, 1092–1102.
- Fernández, T., Harmony, T., Rodríguez, M., Bernal, J., Silva, J., Reyes, A., and Marosi, E. (1995). Eeg activation patterns during the performance of tasks involving different components of mental calculation. *Electroencephalography and clinical neurophysiology* **94**, 175–182.
- Granger, C. W. (1969). Investigating causal relations by econometric models and cross-spectral methods. *Econometrica: journal of the Econometric Society* pages 424–438.
- Granger, C. W. J. (1963). Economic processes involving feedback. *Information and control* **6**, 28–48.
- Gray, R. M. (2011). *Entropy and information theory*. Springer Science & Business Media.
- Guerrero, M. B., Huser, R., and Ombao, H. (2021). Conex-connect: learning patterns in extremal brain connectivity from multi-channel EEG data. *arXiv preprint arXiv:2101.09352*.
- Harmony, T. (2013). The functional significance of delta oscillations in cognitive processing. *Frontiers in integrative neuroscience* **7**, 83.
- Harmony, T., Fernández, T., Silva, J., Bernal, J., Díaz-Comas, L., Reyes, A., Marosi, E., Rodríguez, M., and Rodríguez, M. (1996). Eeg delta activity: an indicator of attention to internal processing during performance of mental tasks. *International journal of psychophysiology* **24**, 161–171.
- Ince, R. A., Giordano, B. L., Kayser, C., Rousselet, G. A., Gross, J., and Schyns, P. G. (2017). A statistical framework for neuroimaging data analysis based on mutual information estimated via a gaussian copula. *Human brain mapping* **38**, 1541–1573.
- Klimesch, W. (2012). Alpha-band oscillations, attention, and controlled access to stored information. *Trends in cognitive sciences* **16**, 606–617.

- Knyazev, G. G. (2007). Motivation, emotion, and their inhibitory control mirrored in brain oscillations. *Neuroscience & Biobehavioral Reviews* **31**, 377–395.
- Ma, J. and Sun, Z. (2011). Mutual information is copula entropy. *Tsinghua Science & Technology* **16**, 51–54.
- Marschinski, R. and Kantz, H. (2002). Analysing the information flow between financial time series. *The European Physical Journal B-Condensed Matter and Complex Systems* **30**, 275–281.
- Motie Nasrabadi, A., Allahverdy, A., Samavati, M., and Mohammadi, M. R. (2020). *EEG data for ADHD / Control children*. IEEE Dataport.
- Nagler, T., Bumann, C., and Czado, C. (2019). Model selection in sparse high-dimensional vine copula models with an application to portfolio risk. *Journal of Multivariate Analysis* **172**, 180–192.
- Nunez, M. D., Nunez, P. L., Srinivasan, R., Ombao, H., Linquist, M., Thompson, W., and Aston, J. (2016). Electroencephalography (eeg): neurophysics, experimental methods, and signal processing. *Handbook of neuroimaging data analysis* pages 175–197.
- Ombao, H., Von Sachs, R., and Guo, W. (2005). Slex analysis of multivariate nonstationary time series. *Journal of the American Statistical Association* **100**, 519–531.
- Schreiber, T. (2000). Measuring information transfer. *Physical review letters* **85**, 461.
- Shojaie, A. and Fox, E. B. (2022). Granger causality: A review and recent advances. *Annual Review of Statistics and Its Application* **9**, 289–319.
- Sklar, M. (1959). Fonctions de repartition an dimensions et leurs marges. *Publ. inst. statist. univ. Paris* **8**, 229–231.
- Tian, Y., Wang, Y., Zhang, Z., and Sun, P. (2021). Fourier-domain transfer entropy spectrum. *Physical Review Research* **3**, L042040.